GEOPHYSICAL RESEARCH LETTERS, VOL. 28, NO. 2, PAGES 387-390, JANUARY 15, 2001

Absence of short-period ULVZ precursors to PcP and ScP from two regions of the CMB

Steven E. Persh, John E. Vidale, and Paul S. Earle[1]

Department of Earth and Space Sciences, University of California, Los Angeles

Abstract. We present results from a study of the core-mantle boundary (CMB) underneath Mexico, Central America, and the northeast Pacific using core-reflected phases PcP and ScP, which provide a direct means of sampling the deep mantle. Precursor arrivals to these phases produced by reflection from the top of an ultra-low velocity layer (ULVZ) at the base of the mantle would contain information about the thickness of such a layer and the velocity reductions within it. Stacks of these phases from 17 earthquakes recorded by the Northern and Southern California Seismographic Networks do not exhibit coherent or incoherent precursor arrivals from a ULVZ. In precursor time windows, ratios of stack amplitudes to those of the CMB-reflected phases fall below predicted values from published ULVZ models. We conclude that ULVZs, if present in these regions, have V_P and V_S reductions less than 10%, are less than five km thick, or have transitions greater than five km wide at their upper boundaries.

Introduction

The core-mantle boundary (CMB) region has long been of interest due to its importance in geodynamical processes [see *Lay et al.,* 1998, for a review]. Recently, several lines of evidence have indicated the existence of a layer at the base of the mantle with large velocity reductions. Seismic arrivals used to identify such ultra-low velocity zones (ULVZs) include precursors to core-reflected phases (PcP [*Mori and Helmberger*, 1995; *Revenaugh and Meyer*, 1997] and ScP [*Garnero and Vidale*, 1999]); delayed core phases ($SP_{\rm diff}KS$ [*Garnero and Helmberger*, 1996]); and scattered core phases (PKP [*Vidale and Hedlin*, 1998; *Wen and Helmberger*, 1998a]). ULVZs have been modeled with thicknesses 5-50 km and velocity reductions $\delta \ln(V_P)$ = -0.1 to -0.2 and $\delta \ln(V_S)$ = -0.1 to -0.5 [*Garnero and Jeanloz*, 2000], although tradeoffs exist between the thickness and velocity reduction [*Garnero and Helmberger*, 1998] and the V_S component has not been directly observed.

Proposed explanations for the low velocities in ULVZs include partial melting [*Williams and Garnero*, 1996], reactions with core material [*Manga and Jeanloz*, 1996], and partitioning of iron from mantle melt [*Knittle*, 1998]. Discerning the behavior of V_P and V_S independently will help resolve the roles played by these processes.

Fresnel zones of detected ULVZs cover 12% of the CMB, 44% of which has been sampled by the above phases [*Williams et al.*, 1998]. The zones vary laterally in their thickness and velocity contrast [*Garnero et al.*, 1998], which may account for the lack of observation in some regions. Cataloging the extent of ULVZs and the character of lateral heterogeneity is an important task for integrating them into our understanding of core-mantle interactions, the origin of mantle upwellings and the fate of subducted lithosphere.

We investigate two regions of the CMB using core-reflected phases PcP and ScP. The former is the compressional wave reflected at the CMB, and the latter is the conversion from shear to compressional waves upon CMB reflection. High-frequency stacks from regional arrays reduce incoherent noise and enable a search for precursors to these phases. We are unable to detect precursor arrivals above the noise, suggesting that ULVZs may not exist in these regions, or that their thickness, velocity reduction, or gradual (rather than discrete) velocity change render precursors too faint to observe.

Data

We obtained short-period, vertical-component seismograms of 17 earthquakes for which data was available from the Northern and Southern California Seismographic Networks (NCSN and SCSN, respectively). The PcP and ScP phases sample the CMB underneath the northeast Pacific and the Mexico/Central America/Caribbean region (Table 1 and Figure 1). The search criteria used to select the earthquakes from the Harvard Centroid-Moment Tensor catalog were: $5.9 \leq M_{\rm W} \leq 6.5$; depth>50 km; and $30^\circ \leq \Delta \leq 65^\circ$. The lower limit for epicentral distance was chosen because as incidence angle becomes more vertical, the amplitudes of ScP and PcP are reduced, in the latter case as a result of the near match in impedance for P waves between the base of the mantle and the outer core. The upper limit was set lower than that of wide-angle studies [e.g., *Weber*, 1993] in order to avoid high noise levels present early in the P-generated coda and to take advantage of increased sensitivity to fine layering at steeper incidence angles.

We employed two methods of stacking: (i) coherent stacking, in which normalized seismograms are linearly summed; and (ii) envelope stacking, in which envelope functions of the seismograms are summed. In coherent stacks, only energy arriving coherently across the network will sum constructively, so we use them to search for precursor arrivals resulting from reflections off the top of a ULVZ. In envelope stacks, any arriving energy contributes to the stack amplitude, regardless of whether the waveform is consistent across the network. Envelope stacks can be used to search for energy from scattered waves.

We decimated the seismograms to 10 samples/second and lowpass filtered below 0.8 Hz (chosen by testing different

[1]Now at U.S. Geological Survey, NEIC, Denver, Colorado

Paper number 2000GL011607.
0094-8276/01/2000GL011607$05.00

Table 1. Earthquake data

Date (yymmdd)	Lat (°N)	Lon (°E)	Depth (km)	Δ (°)	M_W
910123	52.0	178.9	116	47.8	6.4
910814	54.3	-169.3	299	40.9	6.0
920307	10.2	-84.4	73	38.9	6.5
920313	52.5	-178.9	211	46.5	6.4
920523	13.4	-90.0	63	32.7	6.0
920713	-3.9	-76.6	100	54.5	6.3
920815	5.1	-75.7	127	48.7	5.9
920928	13.4	-90.7	72	32.2	6.0
921219	51.9	158.5	56	59.9	6.0
930912	13.8	-90.5	69	32.1	6.0
931120	60.0	-153.1	120	34.5	5.9
931122	11.7	-86.2	108	36.6	5.9
940410	14.7	-92.0	112	30.4, 34.7	6.0
940503	10.3	-60.8	51	60.6	5.9
950208	4.2	-76.6	69	48.7, 52.8	6.3
950819	5.1	-75.7	125	48.7, 52.8	6.5
950923	10.5	-78.7	73	58.3, 62.5	6.4

Events with two Δ entries were recorded by both Southern and Northern California Seismographic Networks (first value is distance to SCSN). Event 940503 was recorded only by NCSN; all others were recorded only by SCSN.

values to find the range where we could best observe P, PcP and ScP). Each trace was inspected visually, and noisy or glitch-filled traces were removed. We aligned a common feature on the P-waves and stacked them. To stack PcP and ScP, we initially aligned based on their predicted travel time relative to P from IASP91 [*Kennett and Engdahl*, 1991]. For some events, the noise was low enough to pick and align PcP and/or ScP on a subset of the seismograms. This additional alignment reduces waveform distortion produced by travel time variations of the core-reflected phases, so these stacks were used in place of the moveout-based stacks. For the SCSN data, we average ∼120 traces per stack; for the NCSN data, we average ∼290 traces per stack.

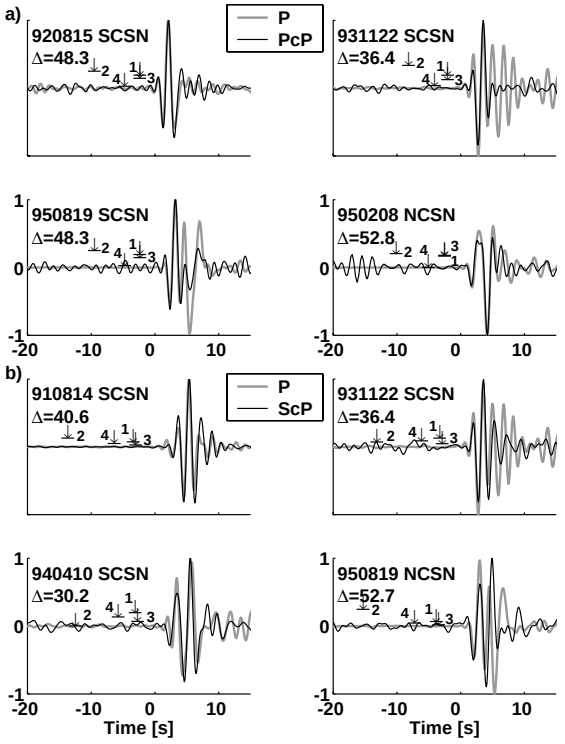

Figure 2. (a) Stacks of PcP for four events overlaid on P-wave stacks. Arrows indicate predicted amplitudes and arrival times of precursors to PcP, obtained by computing reflection coefficients for an P wave incident on a simple discontinuity and converted to an upgoing P wave. The travel time difference from the core-reflection is the time required for the core-reflection to traverse its extra legs within the ULVZ. Both amplitude and time depend on incidence angle, and therefore on epicentral distance range. Model parameters (thickness, $\delta V_P/V_P$, $\delta V_S/V_S$, $\delta\rho/\rho$): 1) (10 km, -0.1, -0.3, 0.0); 2) (40 km, -0.1, -0.3, +0.2); 3) (10 km, -0.1, -0.1, 0.0); and 4) (20 km, -0.1, -0.2, 0.0). (b) As in (a), for ScP.

Observations

From the 17 earthquakes, we produced 21 stacks of PcP and ScP (four events were recorded by both arrays). In one case (931120), we were unable to identify PcP even after stacking; high noise levels made picking P itself on the original traces difficult, so this event is excluded in subsequent discussion. In addition, noise precludes identifying precursors to PcP for events 920313, 921219, 940410 (both networks), and 950923 (SCSN only), so these stacks are excluded. We throw out stacks of two events on which we cannot identify ScP: 920713 and 950923 (SCSN only).

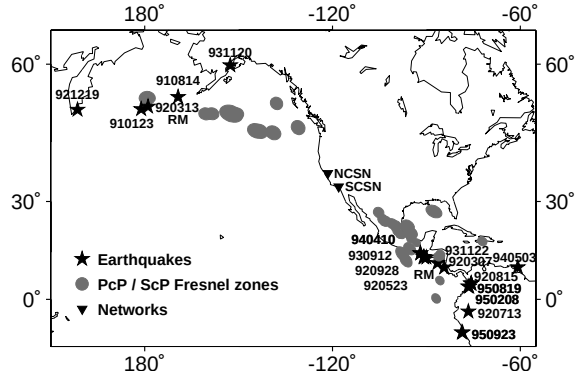

Figure 1. Map showing earthquakes, Northern and Southern California Seismographic Networks (NCSN and SCSN)and core-mantle boundary reflection points for PcP and ScP. The Fresnel zones are computed for a frequency of 0.8 Hz. "RM" indicates approximate centers of regions studied by *Revenaugh and Meyer* [1997]. Areas studied by *Castle and van der Hilst* [2000] coincide with our regions south of the Gulf of Alaska and under eastern Mexico.

Coherent stacks with the best signal-to-noise are shown in Figure 2. The traces are normalized to the amplitude of the core-reflection and overlaid on the P-wave stack for each event, with predicted amplitudes and arrival times of PcP and ScP precursors (PdP and SdP, respectively) shown for four ULVZ models. There is no indication of coherent arrivals above the noise at the times or amplitudes predicted by the models. Background noise allows us only to find upper bounds of allowable structures. The ratio of the average level of background noise to the theoretical precursor amplitude for PdP (for a 15 km-thick ULVZ with $\delta V_P/V_P = -0.1$ and $\delta V_S/V_S = -0.3$) ranges from ∼0.2 to ∼1.9, with four events exceeding 1.0. The noise-to-(predicted SdP) ratios for all but one event range between ∼0.1 and ∼1.7 (six events above 1.0); one earthquake is recorded at ∼46 degrees, where SdP's theoretical amplitude is near zero, which results in an extremely high noise-to-(predicted SdP) ratio. However, even the quietest events, in which the predicted

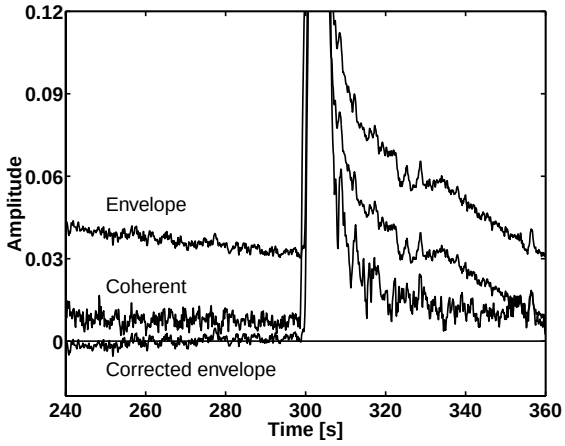

Figure 3. Combined coherent and envelope stacks of ScP from events 910123, 910814 and 920313. The curve labeled "coherent" is an average of envelope functions of the three coherent stacks. The "envelope" curve is an average of envelope stacks, and "corrected envelope" has had a power law fit to the decaying coda subtracted. The amplitude of the ScP pulse at around 300 s is set to 1.0. We do not see a pickup of energy preceding ScP.

amplitude exceeds the background noise by factors of two or more, do not have precursor arrivals.

Figure 3 shows combined envelopes of three of the cleanest events in a time window around ScP, when the background noise has dropped low enough to allow a sensitive search for a pickup of energy before the core-reflection. In the curve labeled "Coherent", we have averaged together envelopes of coherent stacks for the three events; we do this because waveforms from different earthquakes will not necessarily sum constructively. This curve provides further evidence for the lack of a precursor arrival from a constant thickness layer. The upper curve ("Envelope") is an average of the envelope stacks of the three events. In the "Corrected envelope" curve, a power law fit to the decaying P coda of the upper curve has been subtracted. No significant increase in energy precedes ScP, indicating that no extra scattered energy is arriving from a ULVZ.

We can compare the P waveforms to those of the core-reflections to investigate the possibility that scattering or reverberations within the ULVZ distorted PcP or ScP. Generally, PcP and P match quite well (Figure 2). The match with ScP is not as consistent: greater attenuation often renders ScP longer period than P, and it is sometimes difficult to identify common peaks in the arrivals. However, for events 910814 and 920313, the match is near-perfect. In two events (931122 and 950819), P exhibits an extended wavetrain ($\sim$ 5 s) that is significantly reduced in amplitude on the PcP and ScP stacks.

Modeling

In the absence of observed ULVZ reflections, we attempt to place constraints on the properties of ULVZs in the regions of the CMB sampled here. Since the space of possible models is too large to test exhaustively, we chose three representative models for velocity and density changes. For each model, we calculate predicted amplitudes for PdP and SdP at a range of distances by computing reflection coefficients at a simple discontinuity, representing the top of the ULVZ. We assume that effects of attenuation and geometrical spreading are identical for the precursor phases and their corresponding core-reflected phases. High attenuation within the ULVZ would only serve to increase the relative amplitudes of precursors to the core reflections. The difference in their amplitudes is thus attributable to the velocity and density contrasts at the top of the ULVZ (as well as slight variations in properties of the lower mantle). Figure 4 shows the three predicted curves of PdP/PcP and SdP/ScP. For further discussion of amplitude curves for ULVZ-produced arrivals, see *Reasoner and Revenaugh* [in press].

The data amplitude ratios in Figure 4 represent upper bounds for the amplitude of precursory energy to PcP or ScP in our stacks. To obtain the ratios, we identify a time window in which we expect precursor arrivals. The arrival time depends on the height above the CMB of the ULVZ upper boundary, the velocity reductions within it, the epicentral distance, and on which phase we are considering. Therefore we use a variable search window whose start time is a function of epicentral distance and whose duration encompasses possible ULVZ thicknesses between five and 40 km, allowing for velocity reductions of about 0 to 20% for V_P and 10 to 30% for V_S.

We compute envelopes of the coherent stacks and subtract the average noise level in a window preceding the precursor search window for that event and phase. We measure the maximum amplitude within the precursor search window and divide by the maximum PcP or ScP amplitude.

It is clear that no single model adequately describes the behavior of the data. Most of the PdP/PcP data fall below

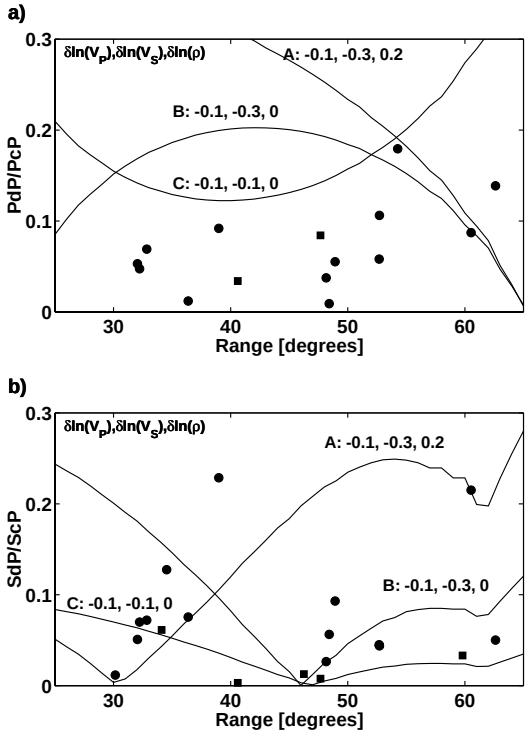

Figure 4. (a) Ratios of stack amplitudes at expected times for precursors to PcP. Data points are maximum measured amplitudes of stacks in expected precursor arrival windows. Squares: northeast Pacific reflection points. Circles: Mexico/Central America/Caribbean reflection points. Curves show predicted amplitudes for three ULVZ models with velocity and density variations indicated. Models: A: *Garnero and Helmberger* [1998] and *Wen and Helmberger* [1998b]; B: *Revenaugh and Meyer* [1997]; C: *Garnero and Vidale* [1999]. (b) As in (a), for ScP.

the predicted amplitudes. The PdP/PcP ratios at greater Δ are less restrictive because of the P-coda noise. The SdP/ScP ratios are generally higher, but also indicate that all models overpredict some observed amplitudes.

Discussion

We do not observe short-period precursors to ULVZs under the northeast Pacific or the Mexico/Central America/Caribbean region. Stacks of PcP and ScP do not contain either coherent arrivals or incoherent scattered energy as precursors, and the good agreement of PcP and ScP waveforms with P suggest that ULVZs in our areas are likely not present, or do not possess the extreme velocity reductions found elsewhere.

At 0.8 Hz, the Fresnel zone for each PcP reflection point spans ∼400 km in diameter; ScP Fresnel zones are about 300 km in diameter. This study primarily samples two regions of the CMB spanning ∼1500-2000 km. We see a consistent absence of ULVZ-generated precursors in both regions, in agreement with the extent of previously reported large-scale regions without ULVZs [*Williams et al.*, 1998].

Alternatively, ULVZs might be present but with diffuse upper boundaries rather than sharp discontinuities. We repeated our calculations of theoretical precursor amplitudes for a ULVZ with a gradational velocity reduction. If the velocity reduction occurs over a vertical scale of 5-10 km (depending on epicentral distance), the amplitude of the precursor is reduced by about half. Another possibility is that the layer is less than a few km thick, in which case it may be too thin for the precursor to be distinguished from the main core-reflection.

Using PcP, *Revenaugh and Meyer* [1997] detect a 8 ± 3 km thick ULVZ south of our southern study area (Figure 1). This can be reconciled with our non-detection if the ULVZ thins to less than 5 km to the north, since we did not allow for thicknesses less than that in our search windows. *Castle and van der Hilst* [2000] found a PREM-like CMB in a region coinciding with our southern study area.

A similar argument can be made for the northern region, where *Revenaugh and Meyer* [1997] find a 11 ± 6 km thick ULVZ slightly west of our study area (Figure 1). $SP_{\mathrm{diff}}KS$ studies also support a ULVZ there [*Garnero and Helmberger*, 1996]. However, this and other ScP studies have not detected one [*Castle and van der Hilst*, 2000; *Vidale and Benz*, 1992].

If ULVZs with V_P reductions around 10% exist in regions where ScP does not detect them, perhaps the common assumption that V_S reductions are three times those of V_P should be reconsidered. There may exist regions in which V_P is sharply reduced but V_S is not. More investigation into the shear wave velocity reductions at the base of the mantle is clearly required.

Acknowledgments. Figure 1 was created using GMT version 3.0 [*Wessel and Smith*, 1995]. We thank Katrin Hafner at SCEC and Rick Lester of USGS for retrieving the network data. Most of this work was supported by NSF grant EAR99-02995, with additional support from EAR00-01126. The manuscript was improved thanks to reviews from John Castle and Ed Garnero.

References

Castle, J. C., and R. D. van der Hilst, The core-mantle boundary under the Gulf of Alaska: No ULVZ for shear waves, *Earth and Planet. Sci. Lett.*, *176*, 311–321, 2000.

Garnero, E. J., and D. V. Helmberger, Seismic detection of a thin laterally varying boundary layer at the base of the mantle beneath the central-pacific, *Geophys. Res. Lett.*, *23*, 977–980, 1996.

Garnero, E. J., and D. V. Helmberger, Further constraints and uncertainties in modeling a thin laterally varying ultralow velocity layer in the lower mantle, *J. Geophys. Res.*, *103*, 12,495–12,509, 1998.

Garnero, E. J., and R. Jeanloz, Fuzzy patches on the Earth's core-mantle boundary?, *Geophys. Res. Lett.*, *27*, 2777–2780, 2000.

Garnero, E. J., and J. E. Vidale, ScP; a probe of ultralow velocity zones at the base of the mantle, *Geophys. Res. Lett.*, *26*, 377–380, 1999.

Garnero, E. J., J. Revenaugh, Q. Williams, T. Lay, and L. H. Kellogg, Ultralow velocity zone at the core-mantle boundary, in *The Core-Mantle Boundary Region, AGU Monograph*, edited by M. Gurnis, M. E. Wysession, E. Knittle, and B. A. Buffett, pp. 319–334, AGU, Washington, D.C., 1998.

Kennett, B. L. N., and E. R. Engdahl, Travel times for global earthquake location and phase association, *Geophys. J. Int.*, *105*, 429–465, 1991.

Knittle, E., The solid/liquid partitioning of major and radiogenic elements at lower mantle pressures: implications for the core-mantle boundary region, in *The Core-Mantle Boundary Region, AGU Monograph*, edited by M. Gurnis, M. E. Wysession, E. Knittle, and B. A. Buffett, pp. 119–130, AGU, Washington, D.C., 1998.

Lay, T., Q. Williams, and E. J. Garnero, The core-mantle boundary layer and deep Earth dynamics, *Nature*, *392*, 461–468, 1998.

Manga, M., and R. Jeanloz, Implications of a metal-bearing chemical boundary layer in D$''$ for mantle dynamics, *Geophys. Res. Lett.*, *23*, 3091–3094, 1996.

Mori, J., and D. V. Helmberger, Localized boundary layer below the mid-pacific velocity anomaly identified from a PcP precursor, *J. Geophys. Res.*, *100*, 20,359–20,365, 1995.

Reasoner, C., and J. Revenaugh, ScP constraints on ultra-low velocity zone density and gradient thickness beneath the Pacific, *J. Geophys. Res.*, in press.

Revenaugh, J., and R. Meyer, Seismic evidence of partial melt within a possibly ubiquitous low-velocity layer at the base of the mantle, *Science*, *277*, 670–673, 1997.

Vidale, J. E., and H. M. Benz, A sharp and flat section of the core-mantle boundary, *Nature*, *359*, 627–629, 1992.

Vidale, J. E., and M. A. H. Hedlin, Evidence for partial melt at the core-mantle boundary north of Tonga from the strong scattering of seismic waves, *Nature*, *391*, 682–685, 1998.

Weber, M., P- and S-wave reflections from anomalies in the lowermost mantle, *Geophys. J. Int.*, *115*, 183–210, 1993.

Wen, L., and D. V. Helmberger, Ultra-low velocity zones near the core-mantle boundary from broadband PKP precursors, *Science*, *279*, 1701–1703, 1998a.

Wen, L., and D. V. Helmberger, A two-dimensional P-SV hybrid method and its application to modeling localized structures near the core-mantle boundary, *J. Geophys. Res.*, *103*, 17,901–17,918, 1998b.

Wessel, P., and W. H. F. Smith, New version of the Generic Mapping Tools released, *Trans. Am. Geophys. Union (EOS)*, *76*, 329, 1995.

Williams, Q., and E. J. Garnero, Seismic evidence for partial melt at the base of Earth's mantle, *Science*, *273*, 1528–1530, 1996.

Williams, Q., J. Revenaugh, and E. J. Garnero, A correlation between ultra-low basal velocities in the mantle and hot spots, *Science*, *281*, 546–549, 1998.

S. E. Persh and J. E. Vidale, Department of Earth and Space Sciences, University of California, Los Angeles, Los Angeles, CA 90095-1567. (e-mail: spersh@moho.ess.ucla.edu)

P. S. Earle, U.S. Geological Survey, MS 967, Box 25046, DFC, Denver, Colorado 80225. (e-mail: paul@earle.org)

(Received March 8, 2000; revised June 15, 2000;
accepted October 17, 2000.)